



Evaluating CALIPSO's 532 nm lidar ratio selection algorithm using AERONET sun photometers in Brazil

F. J. S. Lopes^{1,2}, E. Landulfo², and M. A. Vaughan³

¹Institute of Astronomy, Geophysics and Atmospheric Sciences (IAG), University of São Paulo (USP), São Paulo, SP, Brazil

²Center for Lasers and Application – Nuclear and Energy Research Institute (IPEN/CNEN), São Paulo, SP, Brazil

³NASA Langley Research Center, MS 401A, Hampton, VA, 23681, USA

Correspondence to: F. J. S. Lopes (fabiolopes@usp.br)

Received: 21 December 2012 – Published in Atmos. Meas. Tech. Discuss.: 1 February 2013

Revised: 2 October 2013 – Accepted: 28 October 2013 – Published: 28 November 2013

Abstract. Since the Cloud-Aerosol Lidar and Infrared Pathfinder Satellite Observations (CALIPSO) satellite first began probing the Earth's atmosphere on 13 June 2006, several research groups dedicated to investigating the atmosphere's optical properties have conducted measurement campaigns to validate the CALIPSO data products. Recently, in order to address the lack of CALIPSO validation studies in the Southern Hemisphere, and especially the South American continent, the Lasers Environmental Applications Research Group at Brazil's Nuclear and Energy Research Institute (IPEN) initiated efforts to assess CALIPSO's aerosol lidar ratio estimates using the AERONET sun photometers installed at five different locations in Brazil. In this study we develop a validation methodology to evaluate the accuracy of the modeled values of the lidar ratios used by the CALIPSO extinction algorithms. We recognize that the quality of any comparisons between satellite and ground-based measurements depends on the degree to which the instruments are collocated, and that even selecting the best spatial and temporal matches does not provide an unequivocal guarantee that both instruments are measuring the same air mass. The validation methodology presented in this study therefore applies backward and forward air mass trajectories in order to obtain the best possible match between the air masses sampled by the satellite and the ground-based instruments, and thus reduces the uncertainties associated with aerosol air mass variations. Quantitative comparisons of lidar ratios determined from the combination of AERONET optical depth measurements and CALIOP integrated attenuated backscatter measurements show good agreement with the model values assigned by the CALIOP algorithm. These comparisons yield

a mean percentage difference of $-1.5\% \pm 24\%$. This result confirms the accuracy in the lidar ratio estimates provided by the CALIOP algorithms over Brazil to within an uncertainty range of no more than 30%.

1 Introduction

Aerosols and clouds play an important role in the Earth's radiation budget since their physical and optical properties affect the scattering and absorption processes of solar radiation (Solomon et al., 2007). Clouds act on atmospheric radiation processes by reflecting incoming sunlight back into space and by trapping thermal radiation emitted from the Earth's surface. Aerosols can act to either cool or warm the atmosphere. Cooling occurs when aerosols scatter incoming solar radiation back into space, whereas warming occurs due to the absorption of the incoming sunlight. Moreover, aerosol particles can act as cloud condensation nuclei (CCN) affecting the concentration, size and lifetime of clouds (Anderson et al., 2003; Charlson et al., 1992). Aerosols affect climate processes on both local and global scales, thus representing a large source of uncertainties in the prediction of climate changes, mainly due to their spatial and temporal variability (Anderson et al., 2005). Aerosol optical and physical properties are highly complex, and vary considerably due to differences in their composition, distribution, sources (natural or anthropogenic) and local meteorology. One of the main challenges in the atmospheric sciences lies in acquiring more accurate knowledge about aerosol and cloud properties and how their interactions can affect climate model

predictions. In the last decades, several remote sensing platforms – i.e., spaceborne, aircraft and ground-based measurement systems – have been developed or improved to conduct studies of aerosol and cloud optical properties on local and global scales, as well as to provide the scientific basis for understanding the Earth's climate system. Most of our current understanding of aerosol influences in climate change processes has been developed from the study of horizontal distributions of aerosols derived from space-based passive remote sensor measurements (e.g., the Moderate Resolution Imaging Spectroradiometer (MODIS), Remer et al., 2005). However, since June 2006 the Cloud-Aerosol Lidar and Infrared Pathfinder Satellite Observations (CALIPSO) satellite has retrieved vertical profiles of aerosols and clouds on a global scale, providing important contributions in atmospheric science studies and also complementing our knowledge of the horizontal distributions (Winker et al., 2009, 2010).

The CALIPSO mission is a partnership program developed by the United States' National Aeronautics and Space Administration (NASA) and the Centre National d'Etudes Spatiales (CNES) from France, and has as its principal purpose the retrieval of spatial and optical properties of aerosols and clouds in the vertical profile using the lidar (light detection and ranging) technique. The CALIPSO satellite maintains a 705 km sun-synchronous polar orbit with a velocity of about 7 km s^{-1} . The primary instrument aboard CALIPSO is the Cloud-Aerosol Lidar with Orthogonal Polarization (CALIOP), a two-wavelength laser (532 nm and 1064 nm) operating at a pulse repetition rate of 20.16 Hz (Hunt et al., 2009). CALIOP is an elastic backscatter system, which implies an extra challenge in the retrieval of atmosphere optical properties, since its signals do not contain all of the information required to fully resolve the lidar equation, and therefore aerosol backscatter and extinction coefficients must be retrieved using assumed or modeled values of the so-called extinction-to-backscatter ratio (or lidar ratio – S_{aer}) (Klett, 1985). For this reason, validation methodologies using ground-based instruments are needed to assess the accuracy of both the modeled and the retrieved optical properties reported in the CALIPSO data products.

Since the launch of CALIPSO, several validation studies have been conducted to assess CALIOP's algorithm performance and its data products. These validation studies used different methodologies and approaches, as well as different instruments, including both ground-based and airborne remote sensing systems. Kim et al. (2008) analyzed six cases comparing CALIOP measurements to coincident observations from a ground-based lidar in Seoul, Korea. Several other studies have been conducted comparing CALIOP data products to similar products produced using ground-based elastic backscattering systems (e.g., Tao et al., 2008; Wu et al., 2011) or ground-based Raman lidar systems in the context of EARLINET (Mona et al., 2009; Mamouri et al., 2009; Pappalardo et al., 2010). Ground-based sun photometer measurements (i.e., AERONET) have also been used in

several recent assessments of CALIOP modeled lidar ratios and aerosol optical depths (Schuster et al., 2012; Omar et al., 2013). Other studies have compared CALIOP results to the data products from other satellites. Weisz et al. (2007) used cloud-data products from the Atmospheric Infrared Sounder (AIRS) and MODIS to retrieve estimates of cloud top heights and compare with those obtained using the active sensors such as the Cloud Profiling Radar (CPR) and the CALIOP, onboard the CloudSat and CALIPSO satellites, respectively. Kittaka et al. (2011) compared column aerosol optical depth (AOD) values retrieved by MODIS and CALIOP at 532 nm, showing there is acceptable agreement between the two sensors in ocean regions with low cloudiness, and some differences in the AOD overland. The same study indicated that changes in the selection of the lidar ratio values used in the CALIOP aerosol retrieval would be sufficient to provide a regional mean AOD consistent with that retrieved from MODIS. Some other validation studies used different types of lidar systems onboard aircraft flying in the same trajectory as the CALIPSO satellite. For instance, McGill et al. (2007) qualitatively compared the vertical distribution of clouds measured by CALIOP and the Cloud Physics Lidar (CPL) system onboard NASA's high-altitude ER2 aircraft. Subsequent studies using CPL data by Yorks et al. (2011) and Hlavka et al. (2012) provide quantitative assessments of the CALIOP layer detection scheme and the accuracy of the CALIOP cirrus cloud extinction retrievals, respectively.

Numerous validation studies have been carried out using the NASA Langley Research Center (LaRC) High Spectral Resolution Lidar (HSRL) deployed onboard the Langley B-200 aircraft flying in the same trajectory as the CALIPSO satellite (Burton et al., 2010, 2013; McPherson et al., 2010). Kacenelenbogen et al. (2011) presented a case study using measurements from several instruments – including the LaRC HSRL, the AERONET sun photometers, MODIS, and the POLarization and Directionality of Earth's Reflectances (POLDER) satellite – to compare multiple AOD values with those retrieved by CALIOP. This study suggests that CALIOP consistently underestimates the MODIS AOD values, and investigates possible causes, including CALIOP's low signal-to-noise ratio, cloud contamination, and potentially erroneous values of the aerosol extinction-to-backscatter ratio provided by the CALIOP aerosol models. The most extensive study of CALIOP 532 nm calibration was carried out by Rogers et al. (2011) in a quantitative assessment using LaRC HSRL measurements over and near the North American continent. Comparisons of the 532 nm total attenuated backscatter signal retrieved by both systems showed agreement to within $2.7 \% \pm 2.1 \%$ and $2.9 \% \pm 3.9 \%$ (CALIOP lower) during nighttime and daytime, respectively, indicating the accuracy of the CALIOP 532 nm calibration algorithms.

The vast majority of the ground-based and airborne validation studies have been conducted in the Northern Hemisphere. To our knowledge, the sole exceptions to date are

the global AERONET studies conducted by Schuster et al. (2012) and Omar et al. (2013). There is a distinct lack of CALIOP validation studies in the Southern Hemisphere, and this is especially notable in the South America region, which is a region directly affected by the South Atlantic Anomaly (SAA). The SAA radiation effects can introduce large errors into the CALIOP calibration procedure, which in turn can lead to misclassification or a failure to detect aerosol layers (Hunt et al., 2009; Powell et al., 2009). The validation methodology developed in this paper is, to the best of our knowledge, the first validation study focusing on the CALIOP products reported over South America. In order to evaluate the accuracy and performance of the CALIOP algorithms, ground-based AERONET sun photometer systems installed at five different locations in the Brazilian territory were used. The coincidence of the measurements between the CALIPSO satellite and the sun photometer system was determined by taking into account both physical and atmospheric conditions. The main objective of this study is to present the first quantitative results of the mean bias of the lidar ratio values of the CALIOP algorithms and the ground-based systems. This first validation of CALIOP data products reported in the South America region is divided as follows. Section 2 describes the instruments and their respective data products, i.e., the AERONET sun photometers and the CALIOP system aboard the CALIPSO satellite. The validation methodology is presented in Sect. 3; in this section we also present the family of algorithms created for the validation analysis and enumerate the necessary conditions for obtaining valid comparisons between the data from the three systems. Comparisons of assigned, derived and measured quantities are presented in Sect. 4 and then discussed in the context of other validation studies in Sect. 5.

2 Instruments

This study evaluates the performance of the CALIOP aerosol optical properties retrieval. We focus mainly on the lidar ratio values assigned by the CALIOP algorithms using a data set derived from the AERONET photometers. In this section we present the relevant details of both instruments.

2.1 AERONET sun photometer

The Aerosol RObotic NETwork (AERONET) (Holben et al., 1998) is an international system of ground-based sun photometers that provides automatic sun and sky scanning measurements. Using direct sun measurements, AERONET provides both AOD and the Ångström exponent (\AA), which gives the wavelength dependence of the AOD. By using multiangular and multispectral measurements of atmospheric radiances and applying a flexible inversion algorithm (Dubovik and King, 2000), the AERONET data can also provide several additional aerosol optical parameters, such as size distributions,

single-scattering albedo and refractive index. The operating principle of this system is to acquire aureole and sky radiance observations using a large number of solar scattering angles through a constant aerosol profile, and thus retrieve the aerosol size distribution, the phase function and the AOD. Because sun photometers do not make range-resolved measurements, all of the AERONET derived parameters must be considered as column integrals of their respective altitude-distributed quantities. The channels used are centered at 340, 440, 500, 670, 870, 940 and 1020 nm, with a 1.2° full-angle field of view (FOV). The measurements are taken by pointing the instrument directly at the sun or elsewhere in the sky in nine standard angular intervals employed uniformly by the AERONET network (Holben et al., 1998). The sun photometer is calibrated periodically, either by a remote computer or locally under the supervision of the AERONET network. The calibration methodology assures a coefficient error less than 5%; nonetheless, instrumental variations, calibration, and atmospheric and methodological factors can influence the precision and accuracy of the derived optical thickness, and effectively the total uncertainty in the AERONET AOD is thus about 10% (Dubovik et al., 2000). The inversion of the solar radiances to retrieve AOD values is based on the Beer–Lambert–Bouguer law, given by Eq. (1), assuming that the contribution of multiple scattering within the FOV of 15 the photometer is negligible.

$$I_\lambda = I_{0,\lambda} \exp \left[- \frac{\tau_\lambda}{\mu_s} \right] \quad (1)$$

I_λ and $I_{0,\lambda}$ are the solar irradiances at the top of the atmosphere and at ground level, respectively, and μ_s is the cosine of the solar zenith angle. τ_λ is the path-integrated atmospheric optical depth due to the molecular (Rayleigh) (τ_λ^m) and aerosol ($\tau_\lambda^{\text{aer}}$) scattering, as well the ozone and water vapor absorptions at 670 nm and 870 nm, $\tau_\lambda^{\text{O}_3}$ and $\tau_\lambda^{\text{H}_2\text{O}}$. The aerosol optical depth at 532 nm is retrieved using Eq. (2), derived from the spectral dependence of the aerosol optical depth in the visible spectrum (Ångström, 1964):

$$\tau_{532}^{\text{aer}} = \tau_{500}^{\text{aer}} \left[\frac{532}{500} \right]^{-\text{\AA}} \quad (2)$$

The Ångström exponent \AA is derived from the measured optical thickness in the blue (440 nm) and red channels (675 nm):

$$\text{\AA} = - \frac{\log \left[\frac{\tau_{440}^{\text{aer}}}{\tau_{675}^{\text{aer}}} \right]}{\log \left[\frac{440}{675} \right]} \quad (3)$$

The AERONET AOD values, together with the layer-integrated attenuated backscatter (IAB) coefficient retrieved from CALIOP, will be employed to obtain the most likely lidar ratio values, which will then be compared with those

assigned by the CALIOP aerosol-subtyping scheme (Omar et al., 2009). This is further explained later in the methodology section (Sect. 3). Moreover, using the single-scattering albedo ($\omega(\lambda)$) and 180° phase function values ($P(180^\circ)$) retrieved from the AERONET inversion algorithm, the backscatter-to-extinction ratio (AERONET lidar ratio – S_{aer}) shown in Eq. (4) can be calculated and compared with the values assigned by the CALIOP algorithms. According to Dubovik et al. (2000), the accuracy of single-scattering albedo is estimated to be 0.03 for dust, biomass burning and water-soluble aerosol types. Furthermore, the phase function is very sensitivity to the particle size. Small errors in angular pointing can lead to significant errors in the sky radiances measured especially for coarse-mode particles.

$$S_{\text{aer}} = \frac{4\pi}{\omega(\lambda)P(180^\circ)} \quad (4)$$

2.2 CALIPSO satellite

The CALIPSO satellite was launched in April 2006, and since then has been an integral part of NASA's A-Train satellite constellation (Stephens et al., 2002). CALIPSO flies in a 705 km sun-synchronous polar orbit with an equator-crossing time of about 13:30 local solar time, covering the whole globe in a repeat cycle of 16 days (Winker et al., 2009). The CALIPSO payload consists of three co-aligned nadir-pointing instruments designed to operate autonomously and continuously. Two of these are passive sensors that provide a view of the atmosphere surrounding the lidar curtain, namely a wide-field-of-view camera (WFC) with a pixel spatial resolution of 125 m (Pitts et al., 2007) and a three-channel infrared imaging radiometer (IIR) with a spatial resolution of 1 km and a swath of 61 km (Garnier et al., 2012). The primary instrument is CALIOP, a two-wavelength (532 nm and 1064 nm), polarization-sensitive (at 532 nm) elastic backscatter lidar designed to provide global optical properties of aerosol and clouds. More detailed descriptions of the instruments can be found in the literature (Hostetler et al., 2006; Hunt et al., 2009; Winker et al., 2009).

The CALIOP data products are assembled from the backscatter signals measured by the receiver system and reported in two categories: level 1 products and level 2 products. Level 1 products are composed of calibrated and geolocated profiles of the attenuated backscatter signal and are separated into three types: the total attenuated backscatter profile at 1064 nm, the total attenuated backscatter profile at 532 nm (i.e., the sum of parallel and perpendicular signals) and the perpendicular attenuated backscatter signal at 532 nm (Hostetler et al., 2006; Winker et al., 2009). The quality and accuracy of the level 1 products, and therefore the level 2 products, depend on the accuracy of the calibration of the 532 nm parallel channel. This calibration process normalizes the measured signal with respect to an atmospheric model (Russell et al., 1979; Powell et al., 2009) at high altitudes. The choice of the altitude range is critically important

in order to obtain a backscatter signal with purely molecular contributions, while simultaneously ensuring sufficient signal-to-noise ratio (SNR) and maintaining a linear detector response. Through version 3 of the CALIPSO data products, the 532 nm parallel channel calibration coefficient has been consistently calculated in the altitude interval of 30–34 km, under the assumption that any stratospheric aerosol contributions are negligible. (We note, however, that Vernier et al. (2009) have demonstrated that the stratospheric aerosol loading in this region can in fact be significant, leading to calibration errors that, depending on season and latitude, may be as large as several percent.) The calibration coefficients for the parallel channel measurements are derived from model temperature and pressure data provided by NASA Global Modeling and Assimilation Office (GMAO), taking into accounting molecular and ozone contributions.

The molecular normalization technique can only be applied to nighttime measurements. The CALIOP daytime measurements are affected by the high solar background, which dominates the pure molecular signal and drastically decreases the SNR in the nighttime calibration altitude range. Thus, in the daytime portion of the orbit, the calibration coefficients are derived by a piecewise linear interpolation scheme that is anchored by values derived from the adjacent nighttime portions of the orbit. Details of successive improvements in the CALIOP daytime calibration procedure are described in Hostetler et al. (2006) and Powell et al. (2008, 2009, 2010). Before starting the calibration procedure, the measured data are filtered in order to identify signal spikes resulting from high-energy protons or cosmic ray events. These extreme noise excursions are detected randomly throughout the orbits; however, they occur most frequently in the SAA (Hunt et al., 2009; Powell et al., 2009). The SSA occurs due to the closest approach of the Van Allen radiation belts to the surface of the Earth. When the CALIPSO satellite passes through the SAA region, the 532 nm photomultipliers can produce radiation-induced current spikes that are as much as two orders of magnitude larger than the pulses produced by single photoelectrons. Individual spikes can adversely affect signal averages in low-signal regions, and multiple pulses can increase the dark noise level, with a corresponding decrease in the SNR (Hunt et al., 2009). The signal spikes from high-energy events can introduce large errors in the calibration procedure. To minimize the impacts of these spikes, a multistep adaptive filtering procedure has been implemented to identify and remove signal outliers prior to processing, and thus ensure adequate SNR within the calibration procedure (Lee et al., 2008; Powell et al., 2009).

The level 2 products are derived from the level 1 products. Three different level 2 products are distributed: layer products, profile products and the vertical feature mask (VMF). Layer products provide spatial locations and the optical properties of aerosol and clouds integrated or averaged in each of the layers detected in the atmosphere. The profile products provide the retrieved backscatter and extinction profiles

wherever layers are detected. The VFM provides a map of cloud and aerosol locations, as well as their types. The level 2 products are generated by a sequence of interrelated algorithms that can be subdivided into three main modules. The first module, the selective iterative boundary locator (SYBIL), uses the level 1 attenuated backscatter profiles to detect cloud and aerosol layers (Vaughan et al., 2009). Once the layer boundaries are located, the cloud–aerosol discrimination (CAD) module uses the IAB coefficients, along with altitude and geophysical location to classify each layer as either aerosol or cloud (Liu et al., 2009). Aerosol layers are further classified into six different subtypes (Omar et al., 2009), while clouds are separated according to ice–water phase (Hu et al., 2009). Perhaps the most significant task performed by the aerosol-subtyping algorithm is to associate each aerosol layer with a modeled lidar ratio that characterizes the assigned aerosol type. The CALIPSO aerosol models employed by this algorithm are based on extensive field measurements from the Shoreline Environmental Aerosol Study (SEAS) experiment (Masonis et al., 2003), theoretical calculations using a discrete dipole approximation (Omar et al., 2009) and on a cluster analysis performed on a global AERONET data set acquired between 1993 and 2002 (Omar et al., 2005).

Six different types of aerosol were identified for use in the CALIOP retrieval scheme: dust, smoke, clean and polluted continental, polluted dust and clean marine. Each aerosol subtype is characterized by a lidar ratio distribution (mean and standard deviation), as shown in Table 1. The aerosol-typing and lidar ratio selection scheme uses quantities derived from the level 1 products, such as the integrated attenuated backscatter at 532 nm and the integrated volume depolarization ratio (i.e., the ratio between the integrated perpendicular and parallel backscatter signals). These parameters are calculated by integrating the signal from the top to the base of each detected aerosol layer. However, these two parameters alone are not sufficient to determine the aerosol type, and thus the algorithm also uses geophysical information such as surface type (e.g., land vs. oceans, deserts vs. snow/tundra regions, etc.) and aerosol layer elevation, since lifting mechanisms can be very specific for different types of aerosol. All these physical and optical parameters are used as input in order to choose the most likely aerosol model and constrain the associated lidar ratio uncertainties (Omar et al., 2009). An accurate classification of the aerosol and cloud layers, and especially their S_{aer} values, is critically important for a successful retrieval of the aerosol and cloud optical properties that comprise the CALIOP level 2 data.

3 Validation methodology

To date, all CALIPSO validation studies using ground-based instruments have relied only on spatial and temporal correlations between CALIOP and the ground-based sensor(s) (Kim

Table 1. CALIPSO aerosol types and their associated 532 nm lidar ratio distributions.

Aerosol type	Lidar ratio
Dust	40 ± 20 sr
Smoke	70 ± 28 sr
Clean Continental	35 ± 16 sr
Polluted Continental	70 ± 25 sr
Polluted Dust	55 ± 22 sr
Clean Marine	20 ± 6 sr

et al., 2008; Mamouri et al., 2009; Mona et al., 2009; Wu et al., 2011). However, this simple correlation does not unequivocally guarantee that both instruments are measuring the same air parcels. Even when one can obtain a statistically significant data set, there will always be uncertainties associated with local variations of the aerosol air mass parcels. In order to reduce these uncertainties, we use transport model trajectories to identify the best possible match between the air masses sampled by CALIOP and the air masses sampled by the ground-based instruments. In this sense, the core of our validation methodology is to define “coincidence” not in terms of the proximity of measurements with respect to one another in time and/or space but instead in terms of the proximity of the measurements with respect to a single air mass whose location may be spatially and temporally varying. We accomplish this by using transport models to generate backward or forward trajectories, as required, to ensure that the air/aerosol parcel measured at the validation site is, to the best of our ability, the same the air/aerosol parcel measured by the CALIPSO lidar, similar to the approach taken by Wandinger et al. (2010). By requiring that the instruments probe the same air mass, rather than possibly different but nearby (in time and/or space) parcels, we expect to decrease the fundamental uncertainties introduced by spatial and temporal inhomogeneities. The first step towards the development of our validation methodology was to decide the location (where) and time (when) to collect ground-based data correlated with CALIPSO satellite measurements. Within the Brazilian territory there are several AERONET sites strategically installed in areas that frequently experience large aerosol loadings. For this work we selected a measurement period from 2006 to 2009 for five operational AERONET locations: Rio Branco, Alta Floresta, Cuiabá, Campo Grande and São Paulo. Their geographical coordinates are given in Table 2 and their locations are presented in Fig. 1. These sites are located mainly in the northern and midwestern regions of Brazil, where the dominant vegetation types are savannah and rainforest. These native floras are now interspersed with numerous patches of pasture areas that are highly susceptible to fires during the Brazilian dry season (May–October). These crop-burning activities are responsible for the injection large amounts of biomass burning aerosols into the atmosphere (Artaxo et al., 2002). The presence of a characteristic

Table 2. Geographical coordinates of the five measurement sites used in this study.

Location	Latitude	Longitude
Rio Branco (RB)	9°57'25" S	67°52'08" W
Alta Floresta (AF)	9°52'15" S	56°06'14" W
Cuiabá (CB)	15°43'44" S	56°01'15" W
Campo Grande (CG)	20°26'16" S	54°32'16" W
São Paulo (SP)	23°33'38" S	46°44'23" W

type of aerosol loading in the atmosphere can help in the validation process. In this regard, however, the São Paulo site, located in the southeastern region of Brazil, presents challenges in the analysis of measurements. Given the number of distinct aerosol sources within the city, combined with those brought by long- and mid-range regional transport, the São Paulo atmosphere is frequently filled by an amalgam of many different types of aerosols (Miranda and Andrade, 2005; Landulfo et al., 2008).

3.1 Conditions for coincident measures selection

According to Anderson et al. (2003), when comparing ground-based instruments and a spaceborne lidar, good correlations ($r > 0.9$) occur for time and space offsets less than 3 h and 60 km, and acceptable correlations ($r > 0.8$) occur for time and space offsets less than 6 h and 120 km. In a similar study comparing aerosol optical depths from MODIS and AERONET, Kovacs (2006) demonstrates that the correlation decreases by about 20 % for 200 km and 10 % for 140 km of distance. Thus, in order to match the CALIOP data with ground-based measurements in the Brazilian territory we used the following procedure based on the correlation results presented in the two previous sections. The COVERLAI (CALIPSO overpass locator algorithm) was set up to select all days for which the CALIPSO satellite overflew the five ground sites within a horizontal range distance of $\Delta D \leq 100$ km. Subsequently, the MCSA (multi-instrument coincidence selection algorithm) selects all coincident measurements carried out by the ground-based systems, in a temporal matching window of up to 6 h, centered at the closest approach by CALIPSO. These two conditions are applied to minimize the uncertainties due to the spatial and temporal inhomogeneities in the atmospheric observation range. To ensure that all data were cloud-free, we relied on the number of layers detected, as reported in the CALIPSO 5 km resolution level 2 cloud layer products (Powell et al., 2011), using the algorithm CLARA (cloud–aerosol reader algorithm). The CALIPSO level 2 5 km layer products report a set of spatial and optical properties (e.g., optical depth, layer base and top heights, etc.) for each individual feature detected within the vertical column of atmosphere. To select all coincident measurement days when both CALIOP and AERONET detected cloud-free conditions at the time of the closest approach, the



Fig. 1. Map of Brazil showing the five sites used in this validation study. The Rio Branco site (RB) is located in the northern region of Brazil, and Alta Floresta (AF), Cuiabá (CB) and Campo Grande (CG) are located in the midwestern region. The primary vegetation in all four of these regions is either savannah or rainforest, and can thus be considered as sources of biomass burning aerosol. São Paulo (SP) is located in the southeastern region of Brazil, which is heavily industrialized and whose atmosphere can contain many different types of aerosols.

Number Layers Found product (NLF) is analyzed. The NLF product, which specifies the number of cloud layers detected for each 5 km resolution profile, was inspected for a spatial range of 100 km centered at the closest distance between CALIOP ground-track and the AERONET site (i.e., 20 consecutive 5 km profiles). Those cases for which the NLF product was uniformly zero were flagged as cloud-free-condition measurements. Since the objective of this study is to evaluate aerosol lidar ratio, all aerosol layers from the 5 km resolution aerosol layers products in spatial ranges flagged as cloud-free conditions were selected for analysis. We then inspected the CAD score for the selected aerosol layers. The CALIOP CAD algorithm discriminates between clouds and aerosols using probability distribution functions (PDFs) based on the differences in the optical and physical properties of aerosols and clouds (Liu et al., 2009). The CAD score is reported in the 5 km layer products and provides a numerical confidence level for the classification of layers by the CALIOP CAD algorithm. For this study we selected only those aerosol layers flagged with CAD scores between -50 and -100 , where the larger the magnitude of the CAD score, the higher the numerical confidence level for the classification of each layer detected by the CALIOP system (Liu et al., 2009). This test ensures the selection of reliable aerosol layers. Once we have selected all cloud-free cases and identified all the aerosol 5 km resolution profiles with acceptable CAD score values, we used both the aerosol layer products and the aerosol profile products to calculate the so-called backscatter centroid. This quantity represents the altitude associated with the “backscatter center of mass” (BCM) for the aerosol

layer detected, and is computed using Eq. (5) (Vaughan et al., 2006), where x_i is the total attenuated backscatter signal at 532 nm at altitude Z_i :

$$BCM = \frac{\sum_{i=1}^N x_i Z_i}{\sum_{i=1}^N x_i} \quad (5)$$

The level 2 aerosol layer products are used to determine layer top and bottom height used in the centroid calculation. The backscatter centroids are employed as input altitude data for the air mass trajectories subsequently computed using the HYSPLIT model (Draxler and Hess, 1998). Since the mesoscale variation and short lifetime of aerosols in the troposphere should be taken into account when comparing AOD measurements, we use HYSPLIT trajectory modeling to investigate how the air mass parcels in the CALIPSO ground track region have moved with respect to the AERONET site. By using these trajectory models to better predict the motion of the air masses, we expect to improve the correlation between the optical properties (i.e., AOD and S_{aer}) measured at possibly different times by two different instruments separated spatially. Forward or backward trajectories and the appropriate model vertical velocity option are selected on a case-by-case basis. The starting time of the trajectories is set based on the time of CALIPSO’s closest approach to the AERONET site, and the total trajectory run time is set to 6 h to guarantee at least acceptable air mass matching between CALIOP and the ground-based systems. Trajectories were initiated at the footprint latitude/longitude of the temporal midpoint of each 5 km CALIOP layer datum and the altitude determined by the backscatter centroid Eq. (5). While the application of trajectory analysis decreases the available number of correlative measurements, it simultaneously strengthens the results retrieved from optical properties comparisons of both systems because it increases the likelihood of similar air parcels being probed by the ground instruments and CALIOP. Figure 2 shows the flowchart of the validation methodology algorithms, the data used as input and their output products.

3.2 Comparison of the optical properties – lidar ratio

After producing a merged data set satisfying all the imposed constraints, the IAB coefficient at 532 nm, $\gamma'_{CALIOP,532}$, is calculated for each of 20 consecutive 5 km horizontal resolution profiles for the selected validation days. Instead of using the estimates of $\gamma'_{CALIOP,532}$ reported by CALIPSO data products, we chose instead to calculate revised values of $\gamma'_{CALIOP,532}$ using the equation derived by Platt (1973):

$$\gamma'_{CALIOP,532} = \frac{[1 - \exp(-2\eta\tau_{CALIOP,532})]}{2\eta S_{CALIOP,532}} \quad (6)$$

where η is a multiple-scattering factor ($\eta = 1$ for CALIOP version 3 aerosol retrievals) and $\tau_{CALIOP,532}$ and $S_{CALIOP,532}$

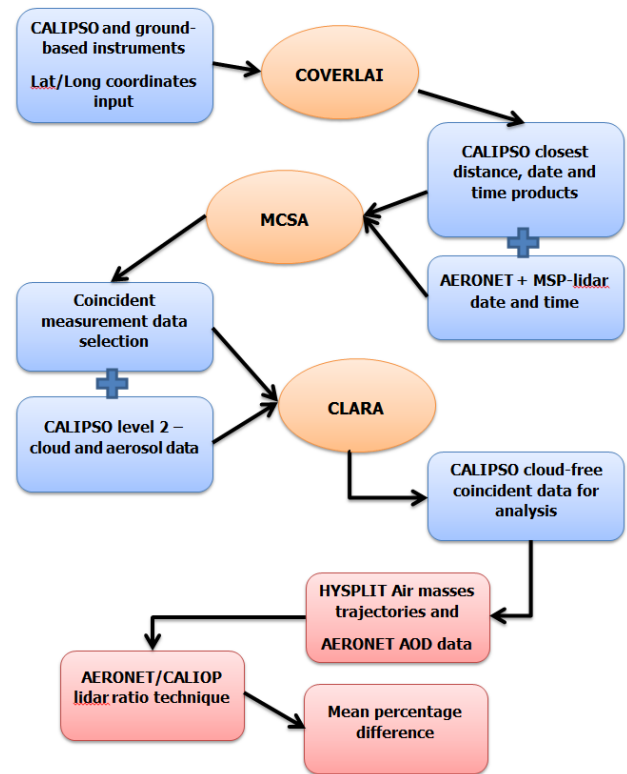


Fig. 2. Flowchart of the validation methodology and their output products.

are respectively the 532 nm aerosol optical depth and the 532 nm final lidar ratio reported in the CALIPSO level 2 aerosol layer products. We found in retrospect that our revised calculation of $\gamma'_{CALIOP,532}$ showed good agreement with estimates of γ'_{532} that are reported in the CALIPSO data product. A rearranged version of Eq. (6) will provide layer lidar ratio estimates for known values of optical depth and integrated attenuated backscatter, and will be used here to retrieve the “appropriate” values of S_{AC} (AERONET/CALIOP lidar ratio) using the AOD values retrieved from the AERONET sun photometers and the value of $\gamma'_{CALIOP,532}$ at 532 nm given by the previous Eq. (6), i.e.,

$$S_{AC} = \frac{[1 - \exp(-2\eta\tau_{AERONET})]}{2\eta\gamma'_{CALIOP,532}} \quad (7)$$

For this study the multiple-scattering factor η will be set to 1, consistent with the value used in the CALIOP version 3 aerosol retrievals. In general, multiple-scattering effects in CALIOP measurements of aerosol layers are thought to be small (Winker et al., 2009), and as such the uncertainties introduced by the approximation of $\eta = 1$ are much smaller than the uncertainties in the CALIPSO lidar ratio models (see Table 1). We note, however, that the magnitude of the multiple scattering most likely varies somewhat according to aerosol type and loading. For example, Wandinger et al.

(2010) suggests that in measurements of fresh Saharan dust layers with optical depths greater than ~ 0.2 , multiple scattering can affect the extinction coefficients retrieved from the CALIPSO lidar signals by 10%–40%. On the other hand, Liu et al. (2011) conclude that multiple scattering from moderately dense dust layers (optical depths less than 1) likely introduces uncertainties of 10% or less in the CALIOP extinction and optical depth retrievals. In any case, these findings should not be of great import to this work, as the occurrence of Saharan dust is relatively rare over Brazil, and modeling studies conducted by Winker (2003) show that the multiple scattering from continental aerosols is noticeably less than from dusts. As described earlier, the AERONET AOD at 532 nm is estimated using Eq. (2) and the retrieved aerosol optical depth at 500 nm. The final lidar ratios reported by CALIOP are subsequently compared to the estimates of S_{AC} calculated in this manner in order to determine the performance of aerosol type classification and lidar ratio selection in the Brazilian territory.

3.3 Limitations of the method

The use of backward and forward trajectories to correlate aerosol mass parcels probed by both instruments relies on the determination of the centroid (i.e., BCM) of the attenuated backscattering coefficients within the layer. Applying Eq. (5) for the computation of the backscatter centroids, we can retrieve the altitude associated with the “center of mass” of the attenuated backscatter profile within the aerosol layers. By associating the AOD measured by AERONET with the BCM of the layers detected by CALIOP, we are explicitly assuming that (a) the regions of enhanced scattering identified by the CALIOP layer detection scheme are responsible for the bulk of the AOD measured by AERONET, and (b) that over the relatively short distances examined in this study, the location of this aerosol mass can be adequately parameterized by the BCM altitude.

AERONET optical depths are representative of the optical extinction from the top to the bottom of the atmosphere without distinguishing between or separating out contributions from different aerosol layers. We therefore consider only those cases where the aerosol detected in the column by CALIOP is all classified as a single type. In CALIOP's multi-grid data-averaging scheme (Vaughan et al., 2009), vertically adjacent features detected at different averaging resolutions are not merged into single layers. These features are instead classified and reported separately in the CALIPSO data products. While this strategy was designed to enable the vertical separation of layers of disparate types (e.g., aerosol above cloud), there can also be cases when a single but diffuse and spatially inhomogeneous layer is detected as a sequence of layer fragments, with vertically adjacent fragments being detected at different averaging resolutions. Thus what might initially appear to be a multilayer scene based on the data reported in the CALIOP layer products is sometimes a single

layer of one type of aerosol with an inhomogeneous vertical distribution of attenuated backscatter coefficients that results in various portions of the layer being detected at different resolutions. Thus to avoid any misleading results in the validation process we have omitted all the multilayer cases where CALIOP identifies two or more different aerosol types within a single column. To merge CALIOP layer fragments of the same aerosol type into a single layer we use the following procedure. We first established the boundaries of a single layer, having its top at the highest top of the multiple layers and its base at the lowest base. We then used the CALIOP level 1 data to recalculate the scattering centroid and the integrated attenuated backscatter for this newly synthesized single aerosol layer. These new centroids were subsequently used to run the HYSPLIT trajectories.

The AERONET AOD values were applied to these new merged layers and to all CALIOP-detected single layers to obtain an empirically derived estimate of the layer lidar ratio. These empirical values are subsequently compared to the model lidar ratios assigned to the individual layers by the CALIOP scene classification algorithms. The technique of ascribing column AOD values measured by passive sensors to aerosol layers detected by lidar measurements is not new (e.g., Welton et al., 2000; Pelon et al., 2002; McGill et al., 2003; He et al., 2006). In a fairly recent study, Burton et al. (2010) compared the extinction coefficients retrieved from CALIOP using the combination of active and passive measurements to the extinction coefficients retrieved using the LaRC HSRL and MODIS instrument data. The analyses of Burton et al. (2010) demonstrate that when a sufficiently accurate column AOD constraint can be obtained (e.g., such as would be provided by MODIS retrievals or AERONET measurements), the assumption of a constant lidar ratio yields relative uncertainties in the CALIOP extinction coefficient profiles that are commensurate with the original pre-mission specification of 40% (Winker et al., 2009). For measurements over land where the HSRL extinction exceeds 0.02 km^{-1} , the study of Burton et al. (2010) showed that the CALIOP extinction profiles retrieved using MODIS AOD as constraint agree with the HSRL extinction profiles to within $\pm 0.0016 \text{ km}^{-1} \pm 20\%$ for two-thirds of all cases. The constant lidar ratios used in the study of Burton et al. (2010) were obtained by requiring that the integral of the extinction profile retrieved from the lidar measurements matched the column AOD obtained from coincident passive sensor measurements (MODIS), i.e., by applying a variant of the same technique used in this study. For our study, AOD values retrieved by AERONET are matched to integrated attenuated backscatter values measured by CALIOP, thus allowing us to derive lidar ratio estimates (S_{AC}) for the aerosol layers. The use of the lidar ratios obtained in this way ensures that the CALIOP AOD estimate and the AERONET AOD measurement match to within the combined uncertainties of the CALIOP IAB and AERONET AOD.

It is important to note that uncertainties associated with vertical inhomogeneities and the horizontal variability of aerosol air masses will apply to some degree to any validation approach that employs instruments that are separated in time and space. The technique we describe here – i.e., air mass matching via backward and/or forward trajectory analysis – represents an attempt to minimize these uncertainties by better ensuring that the same aerosol and same aerosol loading is measured by the two sensors.

4 Results

The challenge in implementing this validation methodology is to establish rigorous criteria for selecting the coincident observations between CALIOP and the ground-based systems that satisfy an optimal spatial–temporal matching window, while simultaneously obtaining a sample size sufficient to yield consistent and statistically significant results. In this section we briefly examine the trade-offs made to maximize our validation sample size, and then compare the extinction-to-backscatter ratios assigned by CALIOP aerosol-subtyping system to those retrieved using the AERONET/CALIOP model (AC model).

4.1 Data selection method

We initially determined all the CALIPSO overpasses lying within a horizontal distance of 55 km or less from the five AERONET sites. Subsequent application of the COVERLAI/MCSA algorithm yielded 161 daytime CALIPSO measurements suitable for comparison to the sun photometer AOD data. One consequence of this filtering scheme was to entirely eliminate data of three sites (AF, CB and SP). The second step was to constrain the coincident measurements to fall within a temporal window up to 6 h from the time of the satellite's closest approach. Doing so further reduced the sample size to a total of 85 correlative daytime measurements, as shown in Table 3. Because the spatial constraint of $\Delta D \leq 55$ km contributed to such a large decrease in the number of coincident samples, we chose to increase the horizontal distance range to $\Delta D \leq 100$ km, which still satisfies the acceptable correlation distance developed by Anderson et al. (2003). As a result, the CALIPSO and AERONET measurement coincidences increase from 85 to 237 days, as shown in Table 4, corresponding to a gain of about 179%. For unknown reasons, some data are not available in the CALIPSO subset pool and thus the initial 237 merged measurements were ultimately limited to a total of 210 measurements.

Table 3. AERONET correlative measurement days for CALIOP closest approach distances less than 55 km.

Station/Year	2006	2007	2008	2009	Total
RB	11	09	08	17	45
AF	0	0	0	0	0
CB	0	0	0	0	0
CG	0	10	15	15	40
SP	0	0	0	0	0
Total	11	19	23	32	85

4.2 Cloud-free conditions for aerosol layers and air mass trajectories

As explained earlier, the backscatter centroids of the selected aerosol layers were used to initiate HYSPLIT air mass trajectories that would indicate when the air masses measured by CALIOP were measured at the AERONET sites. Figure 3 shows the HYSPLIT air mass trajectories plotted for 14 July 2009 at the Alta Floresta AERONET site. In this plot one can see the backward trajectories (in red) that were initiated at the CALIPSO footprint coordinates at 17:41 UTC (i.e., the time of CALIPSO's closest approach). According to the trajectory time histories, the aerosol parcels measured by the AERONET sun photometer at $\sim 15:00$ UTC were transported to the CALIOP overpass region a bit under 3 h later (i.e., at about 17:41 UTC). In this case, the AERONET AOD (τ_{AERONET}) applied in Eq. (7) is the AOD retrieved by the sun photometer around 15:00 UTC. Figure 4 shows the HYSPLIT air mass forward trajectories plotted for 26 May 2007 at the São Paulo AERONET site. The forward trajectories are plotted starting at 17:00 UTC (i.e., around the time of the closest approach of the CALIPSO satellite at 17:08 UTC). The air mass parcels are transported towards the São Paulo AERONET site arriving at $\sim 20:00$ UTC. Once again, the AOD used in Eq. (7) is the AOD retrieved by the AERONET measurement closest to 20:00 UTC. Such a rigorous selection procedure considerably decreases the correlative measurements data set, although it increases the probability that both satellite and ground-based systems are measuring the same aerosol parcels, thus increasing the reliability of the comparisons. In total, this trajectory-based validation procedure identified a merged data set of 75 days having correlative measurements that met the criteria for the comparison of aerosol optical properties. After excluding those cases where CALIOP reported the presence of multiple aerosol types within a single column, the final data set was reduced to $\sim 17.3\%$ of the initial pool of coincident measurements acquired during the daytime for horizontal distances less than or equal to 100 km, as shown in Table 5.

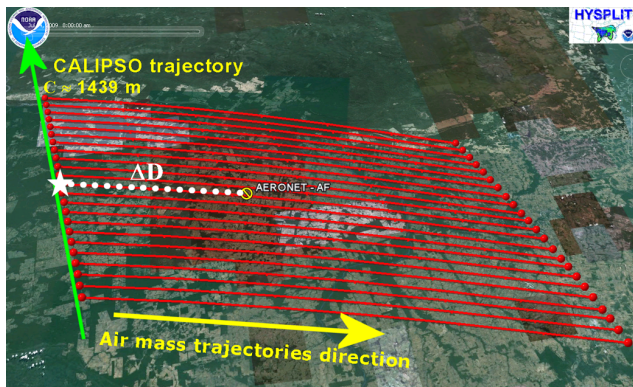


Fig. 3. HYSPLIT backward trajectories in the region of the Alta Floresta AERONET site for 14 July of 2009. The backward trajectories start around the time of CALIPSO's closest approach, at 17:41 UTC. ΔD is the closest distance between CALIPSO trajectory and the AERONET site, in this case 67.3 km. The initial lat/long coordinates have been used as the central values of lat/long for each 5 km horizontal resolution aerosol-layer profiles. The initial altitude for each trajectory, i.e., the backscatter centroids, was in this case 1439 m.

4.3 Lidar ratio from AERONET/CALIOP method

In the initial steps of our comparison we calculated $\gamma'_{\text{CALIOP},532}$ for all single aerosol layers detected in each of 20 consecutive 5 km horizontal resolution profiles, represented by red spheres at the beginning of the trajectories shown in Figs. 3 and 4. After determining the air mass arrival time at the AERONET site, we then applied Eqs. (2) and (3) to the AERONET AOD values for 440 nm and 675 nm to derive estimates of τ_{532}^{aer} . These two quantities, $\gamma'_{\text{CALIOP},532}$ and τ_{532}^{aer} , were retrieved by CALIOP and AERONET sun photometer, respectively. From each pair of values we calculated revised lidar ratio estimates, S_{AC} , by applying the relation presented in Eq. (7). Figure 5 compares the probability distribution functions for S_{AC} to the final lidar ratio values reported in the CALIPSO aerosol data products. In Fig. 5, the CALIOP final lidar ratio distribution shows a high frequency of fixed lidar ratio values at 20 sr (clean marine aerosol type), 35 sr (clean continental), 40 sr (dust), 55 sr (polluted dust) and 70 sr (smoke and polluted continental). Other CALIOP values occur when the initial $S_{\text{CALIOP},532}$ assigned by the CALIOP algorithms is too large, and must be lowered in order to obtain a physically meaningful extinction solution (Young and Vaughan, 2009). A high frequency of fixed $S_{\text{CALIOP},532}$ values is thus expected, since the CALIOP retrieval algorithms use only a small set of fixed lidar ratio values. On the other hand, the lidar ratio values retrieved by the AC method show a continuous distribution spanning all of the CALIOP values. Peaks in the S_{AC} distributions can be seen around 20, 35, 40, 55, 60 and 70 sr. Because the CALIOP model values include uncertainties that range between 35 and 50 %, depending on aerosol type, we consider

Table 4. AERONET correlative measurement days for CALIOP closest approach distances less than 100 km.

Station/Year	2006	2007	2008	2009	Total
RB	11	09	08	17	45
AF	13	19	17	37	86
CB	13	14	13	05	45
CG	0	10	15	15	40
SP	1	15	03	02	21
Total	38	67	56	76	237

Table 5. Percentage of correlative measurements under free-cloud conditions selected for application of the AC method and subsequent comparison to the optical properties retrieved by CALIOP and the AERONET sun photometers.

AERONET Station	Selected days	Total correlative measurements	Percentage
RB	45	8	17.8 %
AF	86	12	14.9 %
CB	45	5	11 %
CG	40	6	15 %
SP	21	10	47.6 %
Total	237	41	17.3 %

the trends in S_{AC} values to be generally consistent with the lidar ratio models developed for the CALIOP algorithm. The mean percentage difference (MPD) between the CALIOP model and AC retrieved lidar ratios is $-2.2 \% \pm 38 \%$, calculated using the follow relation:

$$\text{MPD} = \frac{S_{\text{CALIOP},532} - S_{\text{AC}}}{S_{\text{AC}}} [\%]. \quad (8)$$

The high value of the standard deviation is indicative of the large dispersion in the retrieved lidar ratios. In some cases these disagreements can be a consequence of the atmospheric variability during the time of the CALIPSO's closest approach and the time period which the air masses were transported to the AERONET station region. It is also important to note that this is a one-to-many analysis; that is, a single value of AERONET was used to derive S_{AC} for each of 20 consecutive 5 km resolution aerosol profiles (i.e., Eq. 7), as shown in Figs. 3 and 4. Doing this leaves open the possibility that in some cases the two sensors are not measuring the same air mass parcels, as can be seen by the ends of the backward trajectories in the same figures. Furthermore, the extinction profile for any given layer is retrieved using a single range-invariant value of the lidar ratio specified by the CALIOP aerosol-subtyping algorithm. While this may be a valid approximation for a well-mixed atmosphere, it can introduce some uncertainties in those cases when two or more

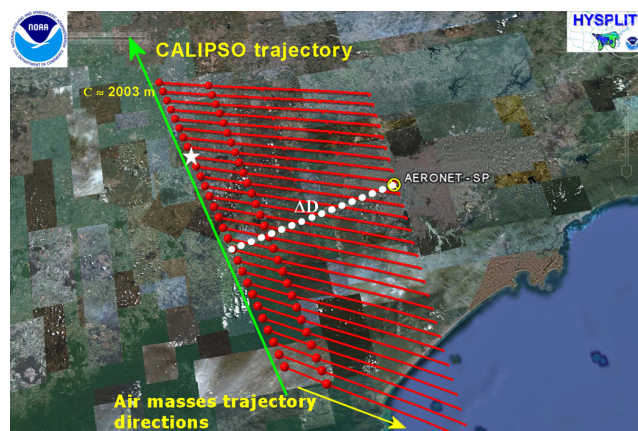


Fig. 4. HYSPLIT backward trajectories in the region of the São Paulo AERONET site for 26 May of 2007. The forward trajectories start around the time of CALIPSO's closest approach (17:08 UTC). ΔD is the closest distance between CALIPSO trajectory and the AERONET site, in this case 71.7 km. The initial lat/lon coordinates have been used as the central values of lat/lon for each 5 km horizontal resolution aerosol-layer profiles. The initial altitude for the trajectories, i.e., the backscatter centroids, was in this case about 2003 m.

aerosol types are present within a single layer identified by CALIOP.

However, when calculating mean percentage differences according to CALIOP aerosol type (see Table 1), the agreement between CALIOP and the AC model is improved. The mean lidar ratio difference is $-9.7\% \pm 13\%$ for dust aerosol type, $-4.7\% \pm 39\%$ for polluted dust, $2.0\% \pm 35\%$ for polluted continental, $7.2\% \pm 40\%$ for smoke and $-6.3\% \pm 20\%$ for clean marine aerosol type, as can be seen in Table 6. All of these mean percentage differences fall within two standard deviations of the CALIOP modeled $S_{\text{CALIOP},532}$. It is also important to note that when applying the same analysis using Eq. (7) for all aerosol layers detected in each of 20 consecutive 5 km horizontal resolution profiles for horizontal range distance of $\Delta D \leq 100$ km, but without taking into accounting the HYSPLIT trajectory modeling to better constraint the comparison between both systems, a mean percentage difference of $-12.3\% \pm 48.7\%$ was found. Both the mean difference and the dispersion are noticeably decreased by application of the air mass matching technique.

The same approach described previously was used to calculate the values of S_{AC} for the single “best matching” 5 km resolution profile. These values were then compared on a one-to-one basis to the lidar ratios assigned by the CALIOP algorithm. This analysis used only those CALIOP profiles connected directly to the AERONET sites by the air mass trajectories obtained from the HYSPLIT model, thus ensuring the greatest probability that both systems have measured the same aerosol parcels. The best matching profiles in Figs. 3

Table 6. Mean percentage lidar ratio difference between the S_{AC} calculation and the CALIOP modeled value $S_{\text{CALIOP},532}$ for each of 20 consecutive 5 km horizontal resolution profiles.

Aerosol type	Mean percentage difference
Dust	$-9.7\% \pm 13\%$
Smoke	$7.2\% \pm 40\%$
Polluted Continental	$2.0\% \pm 35\%$
Polluted Dust	$-4.7\% \pm 39\%$
Clean Marine	$-6.3\% \pm 20\%$

Table 7. Mean percentage lidar ratio difference between the S_{AC} calculation and the CALIOP modeled value $S_{\text{CALIOP},532}$ for the single best matching 5 km horizontal resolution profile.

Aerosol type	Mean percentage difference
Dust	$-5.4\% \pm 24\%$
Smoke	$4.3\% \pm 27\%$
Polluted Continental	$-1.7\% \pm 9\%$
Polluted Dust	$-2.5\% \pm 32\%$

and 4 are designated by a star (*). Figure 6 shows the lidar ratio probability distribution functions for the S_{AC} and the CALIOP aerosol model value for the best matching profiles for each day of correlative measurements. As in the previous analysis, the CALIOP data show high frequencies of fixed lidar ratio values at 20, 40, 55 and 70 sr. Similarly, the S_{AC} retrieval once again shows a broader distribution that spans all of the CALIOP $S_{\text{CALIOP},532}$, with some predominant peaks for dust, around 40 sr; polluted dust aerosol, around 55 sr; and biomass burning or polluted continental aerosol, around 70 sr. The lidar ratio distribution for the best matching profiles yields a mean percentage difference between S_{AC} and the CALIOP modeled value of $-1.5\% \pm 24\%$. In this case, for the best matching profiles, the mean percentage difference between CALIOP and AC model lidar ratios separated according to aerosol type is $-5.4\% \pm 24\%$ for dust, $-2.5\% \pm 32\%$ for polluted dust, $-1.7\% \pm 9\%$ for polluted continental, and $4.3\% \pm 27\%$ for smoke, as can be seen in Table 7. When the lidar ratios are separated according to the modeled CALIOP aerosol types, all percentage differences fall within one standard deviation of the CALIOP model, as shown in Fig. 7.

4.4 Lidar ratio retrieved from AERONET data

To further assess the significance of the lidar ratio differences obtained using the AC model (Sect. 4.3), we used Eq. (4) to calculate S_{aer} values using inversion data from the AERONET retrievals, and then compared the results with the values assigned by the CALIOP algorithm. From a total of 41 correlative measurements between AERONET and CALIOP, there were 33 cases for which AERONET reported

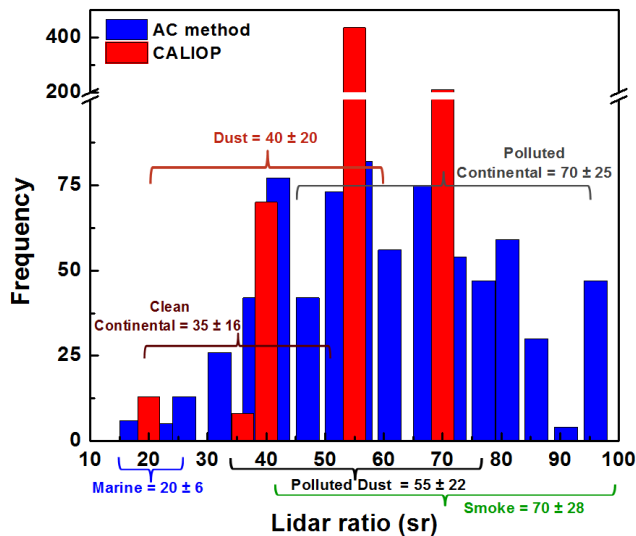


Fig. 5. Lidar ratio occurrence frequencies reported in the CALIPSO data products (red) and those derived using the AC model (blue). The natural variability ascribed to selected CALIPSO aerosol models is shown by the ranges given along the lidar ratio axis. Lidar ratios derived by the AC model are seen to fall entirely within the range spanned by the CALIPSO models.

single-scattering albedo and 180° phase function products (here we consider level 1.5 and level 2 AERONET data). Good agreement between CALIPSO and the AERONET retrievals is found for the different types of aerosols. Mean percentage difference of $-7.3\% \pm 13\%$ is found for polluted dust; $-3.4\% \pm 6\%$ for dust cases; $1.4\% \pm 8\%$ and $2.2\% \pm 7\%$ for polluted continental and smoke aerosol types, respectively; as can be seen in Table 8. In general, the comparison between the two sets of results indicates a relatively small underestimation of the $S_{\text{CALIPSO},532}$ assigned by the CALIPSO scheme, with an overall mean percentage difference of $-3.8\% \pm 11\%$ being derived from all 33 correlative measurements. Since the AERONET level 1.5 data are pre-calibrated and cloud-screened but not post-calibrated, it is more reliable to use only the level 2 data (Holben et al., 1998). Few level 2 data with single-scattering albedo and 180° phase function products were available for these cases. Restricting the analysis to level 2 data, only 9 level 2 correlative measurements are available, from which we obtained a mean difference of $-0.3\% \pm 9\%$, indicating that the CALIPSO assignments slightly underestimate the ground-based retrievals.

5 Discussion and conclusions

The CALIPSO aerosol classification algorithm infers aerosol type, and hence lidar ratio, based on surface type at the lidar footprint, layer-integrated volume depolarization ratio, layer-integrated attenuated backscatter at 532 nm, and layer base

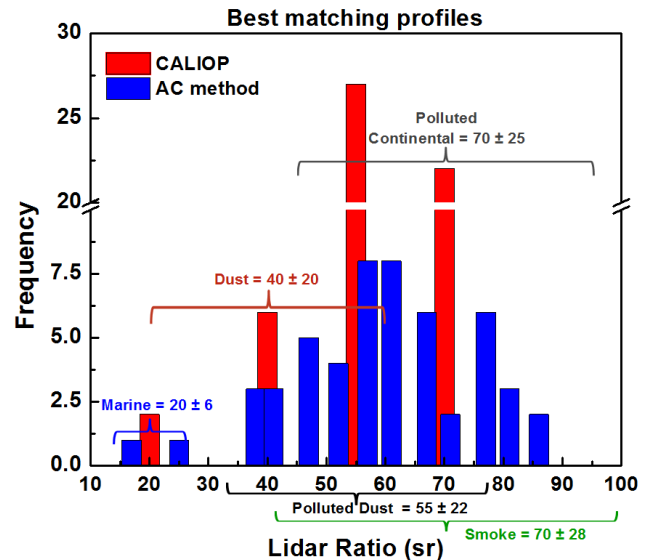


Fig. 6. Lidar ratio occurrence frequencies reported in the CALIPSO data products (red) and those derived using the AC model (blue) for the best matching profile. The natural variability ascribed to selected CALIPSO aerosol models is shown by the ranges given along the lidar ratio axis. Lidar ratios derived by the AC model are seen to fall entirely within the range spanned by the CALIPSO models.

and top heights (Omar et al., 2009). The question we address here is whether the lidar ratios assigned by this classification scheme are in good agreement with the actual lidar ratios of the aerosol layers being measured. In this first quantitative assessment of the performance of the CALIPSO $S_{\text{CALIPSO},532}$ selection algorithm over South America, lidar ratio values were calculated using Eq. (7) for 41 cloud-free coincident measurements of CALIPSO and the AERONET sun photometers. A mean percentage difference of $-2.2\% \pm 38\%$ was obtained by comparing the lidar ratios from the AC calculation with those reported in CALIPSO's 20 consecutive 5 km horizontal resolution profiles. This represents a substantial improvement over the agreement found (a mean percentage difference of $-12.3\% \pm 48.7\%$) when the comparisons were made using the more usual "closest time (or distance)" approach. When using only the best matching profiles indicated by HYSPLIT backward or forward trajectories, the percentage difference decreased to $-1.5\% \pm 24\%$. Comparing these results shows that using model trajectories to correlate measurements between instruments separated spatially and temporally can considerably improve the correspondence between the two separate estimates of the same parameter. This improvement occurs precisely because our validation technique greatly increases the likelihood that the same air mass is probed by both the ground- and satellite-based systems. Comparisons between lidar ratios retrieved from AERONET sun photometer data alone were compared with the model values assigned by the CALIPSO algorithm, and the mean percentage difference is also small, at $-0.3\% \pm 9\%$. These

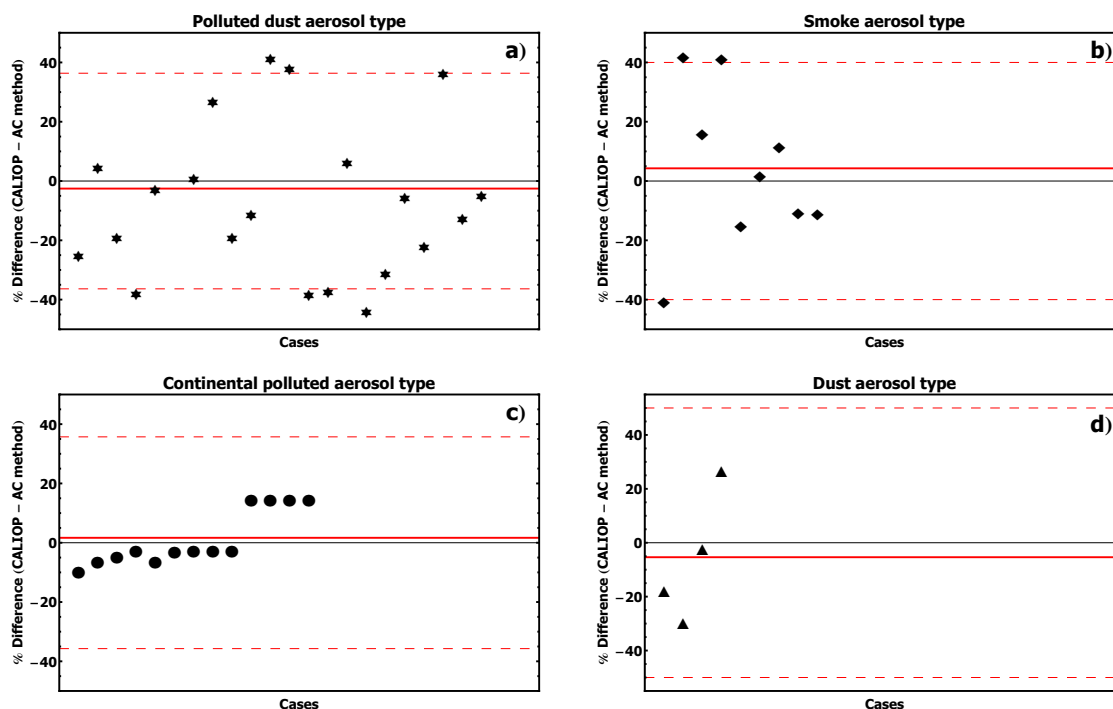


Fig. 7. Lidar ratio mean percentage difference from CALIOP and the AC model separated according to CALIOP aerosol type and using only the best matching profiles approach. The red dashed lines represent one modeled standard deviation, and the red solid line represents the mean percentage difference values (Eq. 8) for each case.

results clearly demonstrate that the a priori lidar ratio values used in the CALIOP algorithms are well suited to the aerosol distributions measured by ground-based systems in Brazilian territory.

Our comparison methodology was developed with the aim of being the first CALIPSO validation study in the SAA region. We expect that this effort will be useful for further aerosol studies in the region and for additional validation of the CALIOP spaceborne lidar, as this location presents a significant challenge to the performance of CALIOP's calibration, layer detection and layer type identification processes, since the SAA noise-induced signal can introduce significant errors in the calculation of the calibration coefficients (Powell et al., 2009). It is important to note, however, that random and systematic uncertainties certainly are present in this methodology. One cannot discount effects that can be related to errors in molecular and aerosol backscatter assumptions in the calibration processes of the AERONET sun photometer systems. However this first validation study in SAA region presents consistent results using different approaches, and it is also consistent with previous studies developed in other regions of the globe using instruments and techniques slightly different from those employed in this study.

In regard to other validation studies, we highlight those conducted under the aegis of EARLINET (Matthais et al., 2009). Mamouri et al. (2009) used a Raman lidar (nighttime) and an elastic backscatter lidar (daytime) to develop

a validation process for the CALIOP 532 nm total attenuated backscatter profiles. This study analyzed 40 coincident measurements within a maximum distance of 100 km between the CALIOP overpasses and ground-based lidar system. These comparisons yielded a mean bias of $-7\% \pm 6\%$ for the total attenuated backscatter profiles for altitudes between 3 and 10 km during clear-sky conditions. Not surprisingly, better agreement was found during the nighttime measurements, at $-4\% \pm 6\%$ versus $-10\% \pm 12\%$ for daytime. However, for the vertical range of 1–3 km the biases were much larger, $-15\% \pm 16\%$ and $-34\% \pm 34\%$ for nighttime and daytime, respectively. This was attributed to the increased horizontal aerosol inhomogeneity in the planetary boundary layer (PBL) region, and suggests that the PBL is ill suited for the application of traditional validation techniques that are restricted to spatial and temporal matching only. Mona et al. (2009) analyzed a total of 68 coincident measurements of level 1, version 2.01 of CALIOP 532 nm attenuated backscatter profiles using a multiwavelength Raman lidar system. From all these cases, 16 nighttime measurements showed a good agreement between the observations of both systems with some differences especially in the boundary layer region and at high altitudes due to the presence of cirrus clouds. Analysis of 11 cases with very clear atmospheric conditions showed mean percentage differences of $-2\% \pm 12\%$ between 3 and 8 km and $-24\% \pm 20\%$ in the PBL, thus offering further evidence that spatial and temporal matching

Table 8. Mean percentage lidar ratio difference between the lidar ratio calculation (S_{AC} and S_{aer}) and the CALIOP modeled value $S_{CALIOP,532}$ for all cases of aerosol type.

Aerosol type	% difference S_{AC} and $S_{CALIOP,532}$ – total profiles	% difference S_{AC} and $S_{CALIOP,532}$ – best matching	% difference S_{aer} and $S_{CALIOP,532}$
Dust	$-9.7 \% \pm 13 \%$	$-5.4 \% \pm 24 \%$	$-3.4 \% \pm 6 \%$
Smoke	$7.2 \% \pm 40 \%$	$4.3 \% \pm 27 \%$	$2.2 \% \pm 7 \%$
Polluted Continental	$2.0 \% \pm 35 \%$	$-1.7 \% \pm 9 \%$	$1.4 \% \pm 8 \%$
Polluted Dust	$-4.7 \% \pm 39 \%$	$-2.5 \% \pm 32 \%$	$-7.3 \% \pm 13 \%$
Clean Marine	$-6.3 \% \pm 20 \%$	–	–

alone are insufficient for PBL validation. Pappalardo et al. (2010) observed a strong dependence on the horizontal distance with a decrease of the correlation coefficient from 0.9 for a distance ≤ 100 km to 0.76 for distances between 100 and 200 km when comparing aerosol backscatter coefficient at 532 nm measured by CALIOP and EARLINET systems. Such studies suggest that differences in the viewing geometries (i.e., up-looking vs. down-looking) and spatial and temporal mismatches between CALIOP and the ground-based Raman lidars, which are exacerbated by the influences of local sources of aerosol and complex terrain between satellite track and ground station, may lead to ambiguous results in the validation comparisons.

Perhaps the most accurate CALIOP validation to date is the comprehensive evaluation conducted by Rogers et al. (2011), which uses the LaRC HSRL aboard an aircraft underflying the trajectory of CALIPSO satellite to assess the CALIOP 532 nm attenuated backscatter profile calibration. This study examines 86 HSRL validation flights of the CALIPSO satellite during both nighttime and daytime in several regions of North America. Comparisons between CALIOP's 532 nm version 3 attenuated backscatter product with HSRL attenuated backscatter profiles found a mean difference of $2.7 \% \pm 2.1 \%$ (CALIOP lower) and $2.9 \% \pm 3.9 \%$ (CALIOP lower) for nighttime and daytime measurements, respectively, including comparisons inside the PBL. While the previously mentioned EARLINET studies (Mamouri et al., 2009; Mona et al., 2009) suggest that CALIOP may be biased low in the PBL, the spatially matched measurements of Rogers et al. (2011) show excellent agreement between the HSRL and CALIOP measurements in this region. When CALIOP data are compared to coincident down-looking HSRL lidar measurements, the PBL variability presented in EARLINET's up-looking comparisons is not detected. Table 9 summarizes some CALIOP validation results obtained by other quantitative studies. These earlier validation studies indicate that CALIOP is well calibrated in the free troposphere region (Mamouri et al., 2009; Mona et al., 2009; Pappalardo et al., 2010). However, results obtained in such studies also point to large differences in comparisons within the PBL region, showing how rapidly the air masses

in this region can change. These changes highlight the importance of employing air mass trajectories in order to reduce the uncertainties in validation comparisons and constrain measurements separated in space and time.

As was the case for the EARLINET studies, the data selected for this validation study were confined almost entirely to the PBL, and the air mass trajectory technique was applied specifically in hopes of avoiding the large discrepancies encountered by the EARLINET researchers. As shown in Sect. 4.3, the use of a single AOD value measured in a single position at the AERONET site and applied to the CALIOP's 5 km resolution aerosol profiles results in good agreement between the AC method and the CALIOP modeled lidar ratio. In our initial analysis, applying a single AERONET AOD to consecutive 5 km resolution CALIOP profiles produced a mean fractional difference of $-2.2 \% \pm 38 \%$ in lidar ratio. The large spread in the results suggests that in some cases the AOD retrieved by the AERONET system applied to the Eq. (7) may not be the most appropriate value, which in turn suggests that the aerosol loading may not be sufficiently homogenous along a 100 km CALIOP ground track. When the same approach is applied to the single CALIOP 5 km profile that is most directly linked to the AERONET site by the HYSPLIT trajectories (i.e., the best matching profile) the mean fractional difference found decreases to $-1.5 \% \pm 24 \%$, thus demonstrating the effectiveness of the trajectory scheme in reducing the variability of the validation comparisons.

When CALIOP's modeled $S_{CALIOP,532}$ are separated by type, the mean percentage lidar ratio difference for each type lies within one standard deviation of the CALIOP models, which suggests that the CALIOP aerosol-typing scheme is reasonably accurate and that the CALIOP models provide a faithful representation of the aerosol types detected in Brazil. If we analyze the results based on CALIOP aerosol type, the dominant aerosol types in the five regions selected in Brazil are polluted continental, defined as continental aerosol with a substantial fraction of urban pollution, and polluted dust, which is defined as a mixture of desert dust and smoke or urban pollution. For both cases we found a consistent agreement between CALIOP lidar ratio

Table 9. Summary of CALIOP validation results from previous studies.

Study	Percentage difference	Data level	Instrument employed
Rogers et al. (2011)	2.9 % \pm 3.9 % 2.7 % \pm 2.1 % CALIOP lower	Level 1–532 nm Total attenuated backscatter	NASA LaRC airborne HSRL system
Kacenenbøgen et al. (2011)	–52.2 % (MODIS) –44.8 % (POLDER) –38.4 % (HSRL) –43.8 % (AERONET)	Aerosol extinction Level 2 product	MODIS POLDER, NASA LaRC airborne HSRL, AERONET
Pappalardo et al. (2010)	4.6 % \pm 50 %	Level 1–532 nm Total attenuated backscatter	Multi wavelength lidar systems
Mona et al. (2009)	–24 % \pm 20 % –2 % \pm 12 %	Level 1–532 nm Total attenuated backscatter	Raman lidar systems
Mamouri et al. (2009)	–15 % \pm 16 % –4 % \pm 6 %	Level 1–532 nm Total attenuated backscatter	Raman lidar systems
This study	–1.5 % \pm 24 % –0.3 % \pm 9 %	Level 2 532 nm lidar ratio	AERONET

selection and the S_{AC} calculated applying the AC method. The mean percentage differences show a small underestimate of CALIOP lidar ratios: $-1.7\% \pm 9\%$ for polluted continental and $-2.5\% \pm 32\%$ for polluted dust. This is illustrated in Fig. 7, where the mean percentage lidar ratio difference lies completely within the expected natural variability (i.e., one standard deviation of the CALIOP model) for polluted continental aerosol, leading to the conclusion that the CALIOP lidar ratio selection scheme is returning accurate results within the South America region. These mean percentage difference values for polluted continental and polluted dust aerosol type are in agreement if we compare with those results obtained by applying the lidar ratio calculated using only AERONET data (Sect. 4.4), i.e. $1.4\% \pm 8\%$ and $-7.3\% \pm 13\%$ for polluted continental and polluted dust, respectively.

Additional studies using more sophisticated measurement techniques (e.g., down-looking airborne HSRL measurements) would be useful in confirming the performance of the CALIOP lidar ratio selection scheme within Brazil. To our knowledge, only one such campaign is currently reported in the literature. Baars et al. (2012) used a multiwavelength Raman Lidar system to show that the predominant aerosol types in the atmosphere of northern and central Brazil are young and aged smokes. The typical mean lidar ratio values of 64 ± 15 sr for the wavelength of 532 nm found by Baars et al. (2012) are in agreement with mean lidar ratio values achieved by the AC method of 71 ± 21 sr for smoke and 69 ± 6 sr for polluted continental. For the other aerosol

types, the vast majority of mean percentage differences fall within one standard deviation, providing further evidence for the accuracy of the CALIPSO automated aerosol classification algorithm.

In the present study, the use of the best matching profile based on the HYSPLIT air mass trajectories analysis decreases the number of possible comparisons between CALIPSO and ground-based instruments. However, the backward and forward trajectories approach proves to be essential in achieving consistent comparisons between the two data sets. The S_{AC} technique defined by Eq. (7) derives estimates of lidar ratio using two independent measurements provided by two entirely different instruments – optical depth measured by AERONET and integrated attenuated backscatter measured by CALIOP. However, the AERONET sun photometers only directly measure optical depths; they specifically do not measure the backscatter component required to directly compute the lidar ratio (i.e., the extinction-to-backscatter ratio). Instead, the AERONET retrieval derives the backscatter component of the lidar ratio by applying Mie scattering theory to the retrieved size distributions and indices of refraction (Dubovik and King, 2000; Dubovik et al., 2000). The accuracy of this backscatter derivation is thus limited by the accuracy of the retrieved size distributions and indices of refraction. As demonstrated by Mamouri et al. (2013), the combination of lidar and photometer measurements can be used to validate the lidar ratio estimates provided by photometer measurements alone. So in effect this

study serves a dual purpose: we validate the performance of the CALIOP lidar ratio selection scheme over Brazil while at the same time providing further validation of the AERONET lidar ratio retrieval scheme.

In summary, it is important to emphasize that this first validation study of the CALIPSO satellite using two different remote sensing instruments in South America is an initial effort to investigate the reliability of the aerosol optical properties retrieved by CALIPSO in the SSA region. Lidar ratio values assigned by CALIOP are in good agreement with those retrieved by the AC method, as well as with those retrieved using the inversion products retrieved from AERONET measurements alone. We therefore conclude that despite the many challenges faced by the CALIOP aerosol-subtyping and lidar ratio selection algorithm, the algorithm works well and shows good accuracy within Brazil. Furthermore, our results demonstrate that air mass trajectories provide a useful and reliable method for properly comparing boundary layer measurements made by CALIOP and ground-based systems and for better constraining measurements that can be widely separated in space and time.

Acknowledgements. The first author wishes to acknowledge the financial support of Fundação para o Amparo da Pesquisa do Estado de São Paulo – FAPESP under project numbers 2013/02357-3, 2011/14365-5, 2011/07475-9 and 2008/58104-8. The authors wish to acknowledge the entire CALIPSO team for their substantial contributions and for the data obtained from the NASA Langley Research Center. They also gratefully acknowledge the team of the AERONET sun photometer network and the PI of each site (Brent Holben, Enio Pereira and Paulo Artaxo), the NOAA Air Resources Laboratory for providing the HYSPLIT transport and dispersion model and the READY website used in this publication, and also the support of Conselho Nacional de Energia Nuclear – CNEN/Brazil.

Edited by: A. Stoffelen

References

- Anderson, T. L., Charlson, R. J., Winker, D. M., Ogren, J. A., and Holmén, K.: Mesoscale variations of tropospheric aerosols, *J. Atmos. Sci.*, 60, 119–136, doi:10.1175/1520-0469(2003)060<0119:MVOTA>2.0.CO;2, 2003.
- Anderson, T. L., Charlson, R. J., Bellouin, N., Boucher, O., Chin, M., Christopherand, S. A., Haywood, J., Kaufman, Y. J., Kinne, S., Ogrenand, J. A., Remer, L. A., Takemura, T., Tanré, D., Torres, O., Trepte, C. R., Wielicki, B. A., Winker, D. M., and Yu, H.: An “A-Train” Strategy for Quantifying Direct Climate Forcing by Anthropogenic Aerosols, *B. Am. Meteorol. Soc.*, 86, 1795–1809, doi:10.1175/BAMS-86-12-1795, 2005.
- Ångström, A.: The parameters of atmospheric turbidity, *Tellus*, 16, 64–75, doi:10.1111/j.2153-3490.1964.tb00144.x, 1964.
- Artaxo, P., Martins, J. V., Yamasoe, M. A., Procópio, A. S., Pauliquevis, T. M., Andrea, M. O., Guyon, P., Gatti, L. V., and Leal, A. M. C.: Physical and chemical properties of aerosols in the wet and dry seasons in Rondônia, Amazônia, *J. Geophys. Res.*, 107, D208081, doi:10.1029/2001JD000666, 2002.
- Baars, H., Ansmann, A., Althausen, D., Engelmann, R., Heese, B., Müller, D., Artaxo, P., Paixão, M., Pauliquevis, T., and Souza, R.: Aerosol profiling with lidar in the Amazon Basin during the wet and dry season, *J. Geophys. Res.*, 117, D21201, doi:10.1029/2012JD018338, 2012.
- Burton, S. P., Ferrare, R. A., Hostetler, C. A., Hair, J. W., Kittaka, C., Vaughan, M. A., Obland, M. D., Rogers, R. R., Cook, A. L., Harper, D. B., and Remer, L. A.: Using airborne high spectral resolution lidar data to evaluate combined active plus passive retrievals of aerosol extinction profiles, *J. Geophys. Res.*, 115, D00H15, doi:10.1029/2009JD012130, 2010.
- Burton, S. P., Ferrare, R. A., Vaughan, M. A., Omar, A. H., Rogers, R. R., Hostetler, C. A., and Hair, J. W.: Aerosol classification from airborne HSRL and comparisons with the CALIPSO vertical feature mask, *Atmos. Meas. Tech.*, 6, 1397–1412, doi:10.5194/amt-6-1397-2013, 2013.
- Charlson, R. J., Schwartz, S. E., Hales, J. M., Cess, R. D., Coakley Jr., J. A., Hansen, J. E., and Hofmann, D. J.: Climate Forcing by Anthropogenic Aerosols, *Science*, 225, 423–430, doi:10.1126/science.255.5043.423, 1992.
- Draxler, R. and Hess, G.: Description of the HYSPLIT 4 modeling system, NOAA Tech. Memo. ERL ARL-224, NOAA Air Resources Laboratory, Silver Spring, MD, USA, available at: <http://ready.arl.noaa.gov/HYSPLIT.php> (last access: 15 May 2011), 1998.
- Dubovik, O. and King, M. D.: A flexible inversion algorithm for retrieval of aerosol optical properties from Sun and sky radiance measurements, *J. Geophys. Res.*, 105, 20673–20696, doi:10.1029/2000JD900282, 2000.
- Dubovik, O., Smirnov, A., Holben, B. N., King, M. D., Kaufman, Y. J., Eck, T. F., and Slutsker, I.: Accuracy assessments of aerosol optical properties retrieved from AEROSOL ROBOTIC Network (AERONET) Sun and sky radiance measurements, *J. Geophys. Res.*, 105, 9791–9806, doi:10.1029/2000JD900040, 2000.
- Garnier, A., Pelon, J., Dubuisson, P., Faivre, M., Chomette, O., Pascal, N., and Kratz, D. P.: Retrieval of cloud properties using CALIPSO Imaging Infrared Radiometer. Part I: effective emissivity and optical depth, *J. Appl. Meteorol. Clim.*, 51, 1407–1425, doi:10.1175/JAMC-D-11-0220.1, 2012.
- Hlavka, D., Yorks, J., Young, S., Vaughan, M., Kuehn, R., McGill, M., and Rodier, S.: Airborne Validation of Cirrus Cloud Properties Derived from CALIPSO Lidar Measurements: Optical Properties, *J. Geophys. Res.*, 117, D09207, doi:10.1029/2011JD017053, 2012.
- He, Q. S., Li, C. C., Mao, J. T., Lau, A. K. H., and Li, P. R.: A study on the aerosol extinction-to-backscatter ratio with combination of micro-pulse LIDAR and MODIS over Hong Kong, *Atmos. Chem. Phys.*, 6, 3243–3256, doi:10.5194/acp-6-3243-2006, 2006.
- Holben, B. N., Eck, T. F., Slutsker, I., Tanré, D., Buis, J. P., Setzer, A., Vermote, E., Reagan, J. A., Kaufman, Y. J., Nakajima, T., Lavenu, F., Jankowiak, I., and Smirnov, A.: Aeronet – A Federal Instrument Network and Data Archive for Aerosol Characterization, *Remote Sens. Environ.*, 66, 1–16, doi:10.1016/S0034-4257(98)00031-5, 1998.
- Hostetler, C. A., Liu, Z., Reagan, J., Vaughan, M. A., Winker, D. M., Osborn, M., Hunt, W. H., Powell, K. A., and Trepte,

- C.: CALIOP Algorithm Theoretical Basis Document – Calibration and level 1 data products. release 1.0, PC-SCI-201 Part 1, NASA Langley Research Center, Hampton, Virginia, USA, available at: http://www-calipso.larc.nasa.gov/resources/project_documentation.php (last access: 10 June 2010), 2006.
- Hu, Y., Winker, D. M., Vaughan, M. A., Lin, B., Omar, A., Trepte, C., Flittner, D., Yang, P., Nasiri, S. L., Baum, B., Holz, R., Sun, W., Liu, Z., Wang, Z., Young, S., Stammes, K., Huang, J., and Kuehn, R.: CALIPSO/CALIOP cloud phase discrimination algorithm, *J. Atmos. Ocean. Tech.*, 26, 2293–2309, doi:10.1175/2009JTECHA1280.1, 2009.
- Hunt, W. H., Winker, D. M., Vaughan, M. A., Powell, K. A., Lucker, P. L., and Weimer, C.: CALIPSO Lidar Description and Performance Assessment, *J. Atmos. Ocean. Tech.*, 26, 1214–1228, doi:10.1175/2009JTECHA1223.1, 2009.
- Kacenenbogen, M., Vaughan, M. A., Redemann, J., Hoff, R. M., Rogers, R. R., Ferrare, R. A., Russell, P. B., Hostetler, C. A., Hair, J. W., and Holben, B. N.: An accuracy assessment of the CALIOP/CALIPSO version 2/version 3 daytime aerosol extinction product based on a detailed multi-sensor, multi-platform case study, *Atmos. Chem. Phys.*, 11, 3981–4000, doi:10.5194/acp-11-3981-2011, 2011.
- Kim, S.-W., Berthier, S., Raut, J.-C., Chazette, P., Dulac, F., and Yoon, S.-C.: Validation of aerosol and cloud layer structures from the space-borne lidar CALIOP using a ground-based lidar in Seoul, Korea, *Atmos. Chem. Phys.*, 8, 3705–3720, doi:10.5194/acp-8-3705-2008, 2008.
- Kittaka, C., Winker, D. M., Vaughan, M. A., Omar, A., and Remer, L. A.: Intercomparison of column aerosol optical depths from CALIPSO and MODIS-Aqua, *Atmos. Meas. Tech.*, 4, 131–141, doi:10.5194/amt-4-131-2011, 2011.
- Klett, J. D.: Lidar inversion with variable backscatter/extinction ratios, *Appl. Optics*, 24, 1638–1643, doi:10.1364/AO.24.001638, 1985.
- Kovacs, T.: Comparing MODIS and AERONET aerosol optical depth at varying separation distances to assess ground-based validation strategies for spaceborne Lidar, *J. Geophys. Res.*, 111, D24203, doi:10.1029/2006JD007349, 2006.
- Landulfo, E., Papayannis, A., Torres, A. S., Uehara, S. T., Pozzetti, L. M. V., de Matos, C. A., Sawamura, P., Nakaema, W. M., and de Jesus, W. C.: A four-year Lidar-sun photometer aerosol study at São Paulo, Brazil, *J. Atmos. Ocean. Tech.*, 25, 1463–1468, doi:10.1175/2007JTECHA984.1, 2008.
- Lee, K.-P., Vaughan, M. A., Liu, Z., Hunt, W., and Powell, K.: Revised Calibration Strategy for the CALIOP 532 nm Channel: Part 1 – Nighttime, Reviewed and Revised Papers Presented at the 24th International Laser Radar Conference, Boulder-Colorado-USA, 23–27 June, 1173–1176, ISBN 978-0-615-21489-4, 2008.
- Liu, Z., Vaughan, M. A., Winker, D. M., Kittaka, C., Getzewich, B. J., Kuehn, R. E., Omar, A. H., Powell, K. A., Trepte, C. R., and Hostetler, C. A.: The CALIPSO Lidar cloud and aerosol discrimination: Version 2 algorithm and initial assessment of performance, *J. Atmos. Ocean. Tech.*, 26, 1198–1213, doi:10.1175/2009JTECHA1231.1, 2009.
- Liu, Z., Winker, D., Omar, A., Vaughan, M., Trepte, C., Hu, Y., Powell, K., Sun, W., and Lin, B.: Effective lidar ratios of dense dust layers over North Africa derived from the CALIOP measurements, *J. Quant. Spectrosc. Rad.*, 121, 204–213, doi:10.1016/j.jqsrt.2010.05.006, 2011.
- Mamouri, R. E., Amiridis, V., Papayannis, A., Giannakaki, E., Tsaknakis, G., and Balis, D. S.: Validation of CALIPSO spaceborne-derived attenuated backscatter coefficient profiles using a ground-based lidar in Athens, Greece, *Atmos. Meas. Tech.*, 2, 513–522, doi:10.5194/amt-2-513-2009, 2009.
- Mamouri, R. E., Ansmann, A., Nisantzi, A., Kokkalis, P., Schwarz, A., and Hadjimitsis, D.: Low Arabian dust extinction-to-backscatter ratio, *Geophys. Res. Lett.*, 40, 1–5, doi:10.1002/grl.50898, 2013.
- Masonis, S. J., Anderson, T. L., Covert, D. S., Kapustin, V., Clarke, A. D., Howell, S., and Moore, K.: A study of the extinction-to-backscatter ratio of marine aerosol during the Shoreline Environmental Aerosol Study, *J. Atmos. Ocean. Tech.*, 20, 1388–1402, doi:10.1175/1520-0426(2003)020<1388:ASOTER>2.0.CO;2, 2003.
- Matthais, V., Freudenthaler, V., Amodeo, A., Balin, I., Balis, D., Bösenberg, J., Chaikovskiy, A., Chourdakis, G., Comeron, A., Delaval, A., De Tomasi, F., Eixmann, R., Hågård, A., Komguem, L., Kreipl, S., Matthey, R., Rizi, V., Rodrigues, J. A., Wandinger, U., and Wang, X.: Aerosol Lidar Intercomparison in the Framework of the EARLINET Project. 1. Instruments, *Appl. Optics*, 13, 961–976, doi:10.1364/AO.43.000961, 2004.
- McGill, M. J., Hlavka, D. L., Hart, W. D., Welton, E. J., and Campbell, J. R.: Airborne lidar measurements of aerosol optical properties during SAFARI-2000, *J. Geophys. Res.*, 108, 8493, doi:10.1029/2002JD002370, 2003.
- McGill, M. J., Vaughan, M. A., Trepte, C. R., Hart, W. D., Hlavka, D. L., Winker, D. M., and Kuehn, R.: Airborne validation of spatial properties measured by the CALIPSO Lidar, *J. Geophys. Res.*, 112, D20201, doi:10.1029/2007JD008768, 2007.
- McPherson, C. J., Reagan, J. A., Schafer, J., Giles, D., Ferrare, R., Hair, J., and Hostetler, C.: AERONET, airborne HSRL, and CALIPSO aerosol retrievals compared and combined: A case study, *J. Geophys. Res.*, 115, D00H21, doi:10.1029/2009JD012389, 2010.
- Miranda, R. M. and Andrade, M. F.: Physicochemical characteristics of atmospheric aerosol during winter in the São Paulo Metropolitan area in Brazil, *Atmos. Environ.*, 39, 6188–6193, doi:10.1016/j.atmosenv.2005.06.055, 2005.
- Mona, L., Pappalardo, G., Amodeo, A., D'Amico, G., Madonna, F., Boselli, A., Giunta, A., Russo, F., and Cuomo, V.: One year of CNR-IMAA multi-wavelength Raman lidar measurements in coincidence with CALIPSO overpasses: Level 1 products comparison, *Atmos. Chem. Phys.*, 9, 7213–7228, doi:10.5194/acp-9-7213-2009, 2009.
- Omar, A. H., Won, J.-G., Winker, D. M., Yoon, S.-C., Dubovik, O., and McCormick, M. P.: Development of global aerosol models using cluster analysis of Aerosol Robotic Network (AERONET) measurements, *J. Geophys. Res.*, 110, D10S14, doi:10.1029/2004JD004874, 2005.
- Omar, A. H., Winker, D. M., Kittaka, C., Vaughan, M. A., Liu, Z., Hu, Y., Trepte, C. R., Rogers, R. R., Ferrare, R. A., Lee, K., Kuehn, R. E., and Hostetler, C. A.: The CALIPSO automated aerosol classification and Lidar Ratio Selection Algorithm, *J. Atmos. Ocean. Tech.*, 26, 1994–2014, doi:10.1175/2009JTECHA1231.1, 2009.
- Omar, A. H., Winker, D. M., Tackett, J., Kar, J., Liu, Z., Vaughan, M., Powell, K., and Trepte, C.: CALIPSO AERONET Aerosol

- Optical Depth Intercomparisons: One Size Fits None, *J. Geophys. Res.*, in review, 2013.
- Pappalardo, G., Wandinger, U., Mona, L., Hiebsch, A., Mattis, I., Amodeo, A., Ansmann, A., Seifert, P., Linné, H., Apituley, A., Arboledas, L. A., Balis, D., Chaikovsky, A., D'Amico, G., De Tomasi, F., Freudenthaler, V., Giannakaki, E., Giunta, A., Grigorov, I., Iarlori, M., Madonna, F., Mamouri, R. E., Nasti, L., Papayannis, A., Pietruczuk, A., Pujadas, M., Rizi, V., Rocadenbosch, F., Russo, F., Schnell, F., Spinelli, N., Wang, X., and Wiegner, M.: EARLINET correlative measurements for CALIPSO: First intercomparison results, *J. Geophys. Res.*, 115, D00H19, doi:10.1029/2009JD012147, 2007.
- Pelon, J., Flamant, C., Chazette, P., Leon, J.-F., Tanré, D., Sicard, M., and Satheesh, S. K.: Characterization of aerosol spatial distribution and optical properties over the Indian Ocean from airborne LIDAR and radiometry during INDOEX '99, *J. Geophys. Res.*, 107, 8029, doi:10.1029/2001JD000402, 2002.
- Pitts, M. C., Thomason, L. W., Hu, Y., and Winker, D. M.: An assessment of the on-orbit performance of the CALIPSO Wide Field Camera, in: *Remote Sensing of Clouds and the Atmosphere XII Proceedings of SPIE, Florence-Italy, 25 October, 675, 67450k*, doi:10.1117/12.737377, 2007.
- Platt, C. M. R.: Lidar and radiometer observations of cirrus clouds, *J. Atmos. Sci.*, 30, 1191–1204, doi:10.1175/1520-0469(1973)030<1191:LAROO>2.0.CO;2, 1973.
- Powell, K. A., Vaughan, M. A., Kuehn, R., Hunt, W. H., and Lee, K.-P.: Revised calibration strategy for the caliop 532-nm channel: Part II daytime, Reviewed and Revised Papers Presented at the 24th International Laser Radar Conference, Boulder-Colorado-USA, 23–27 June, 1177–1180, ISBN 978-0-615-21489-4, 2008.
- Powell, K. A., Hostetler, C. A., Liu, Z., Vaughan, M. A., Kuehn, R. E., Hunt, W. H., Liu, K., Trepte, C. R., Rogers, R. R., Young, S. A., and Winker, D. M.: CALIPSO Lidar Calibration Algorithms Part I: Nighttime 532 nm Parallel Channel and 532 nm Perpendicular Channel, *J. Atmos. Ocean. Tech.*, 26, 2015–2033, doi:10.1175/2009JTECHA1242.1, 2009.
- Powell, K. A., Vaughan, M. A., Rogers, R. R., Kuehn, R., Hunt, W. H., Lee, K.-P., and Murray, T. D.: The CALIOP 532-nm Channel Daytime Calibration: Version 3 Algorithm, Reviewed and Revised Papers Presented at the 25th International Laser Radar Conference, St. Petersburg-Russia, 5–9 July, 1367–1370, 2010.
- Powell, K. A., Vaughan, M. A., Winker, D. M., Lee, K.-P., Pitts, M., Trepte, C., Detweiler, P., Hunt, W., Lambeth, J., Lucker, P., Murray, T., Hagolle, O., Lifermann, A., Faivre, M., Garnier, A., and Pelon, J.: CALIPSO Data Products Catalog, Release 3.4, PC-SCI-503, NASA Langley Research Center, Hampton, VA-USA, available at: http://www-calipso.larc.nasa.gov/products/CALIPSO_DPC_Rev3x4.pdf, 2011.
- Remer, L. A., Kaufman, Y. J., Tanré, D., Mattoo, S., Chu, D. A., Martins, J. V., Li, R. R., Ichoku, C., Levy, R. C., Kleidman, R. G., Eck, T. F., Vermote, E., and Holben, B. N.: The MODIS aerosol algorithm, products, and validation, *J. Atmos. Sci.*, 62, 947–973, doi:10.1175/JAS3385.1, 2005.
- Rogers, R. R., Hostetler, C. A., Hair, J. W., Ferrare, R. A., Liu, Z., Obland, M. D., Harper, D. B., Cook, A. L., Powell, K. A., Vaughan, M. A., and Winker, D. M.: Assessment of the CALIPSO Lidar 532 nm attenuated backscatter calibration using the NASA LaRC airborne High Spectral Resolution Lidar, *Atmos. Chem. Phys.*, 11, 1295–1311, doi:10.5194/acp-11-1295-2011, 2011.
- Russell, P. B., Swisler, T. J., and McCormick, M. P.: Methodology for error analysis and simulation of lidar aerosol measurements, *Appl. Optics*, 18, 3783–3797, 1979.
- Solomon, S., Qin, D., Manning, M., Chen, Z., Marquis, M., Averyt, K. B., Tignor, M., and Miller, H. L.: Contribution of Working Group I to the Fourth Assessment Report of the Intergovernmental Panel on Climate Change, 1st edition, Cambridge University Press, United Kingdom and New York, 996, 2007.
- Schuster, G. L., Vaughan, M., MacDonnell, D., Su, W., Winker, D., Dubovik, O., Lapyonok, T., and Trepte, C.: Comparison of CALIPSO aerosol optical depth retrievals to AERONET measurements, and a climatology for the lidar ratio of dust, *Atmos. Chem. Phys.*, 12, 7431–7452, doi:10.5194/acp-12-7431-2012, 2012.
- Stephens, G. L., Vane, D. G., Boain, R. J., Mace, G. G., Sassen, K., Wang, Z., Illingworth, A. J., O'Connor, E. J., Rossow, W. B., Durden, S. L., Miller, S. D., Austin, R. T., Benedetti, A., Mitrescu, C., and CloudSat Science Team: The CloudSat mission and the A-Train: A new dimension of space-based observations of clouds and precipitation, *B. Amer. Meteorol. Soc.*, 83, 1771–1790, doi:10.1175/BAMS-83-12-1771, 2002.
- Tao, Z., McCormick, M. P., and Wu, D.: A comparison method for spaceborne and ground-based lidar and its application to the CALIPSO lidar, *Appl. Phys. B*, 91, 639–644, doi:10.1007/s00340-008-3043-1, 2008.
- Vaughan, M. A., Winker, D. M., and Powell, K. A.: CALIOP Algorithm Theoretical Basis Document – Part 2: Feature detection and layer properties algorithms. Release 1.01, PC-SCI-202 Part 2, NASA Langley Research Center, Hampton, Virginia, USA, available at: http://www-calipso.larc.nasa.gov/resources/project_documentation.php (last access: 10 June 2010), 2006.
- Vaughan, M. A., Powell, K. A., Kuehn, R. E., Young, S. A., Winker, D. M., Hostetler, C. A., Hunt, W. H., Liu, Z., McGill, M. J., and Getzewich, B. J.: Fully automated detection of cloud and aerosol layers in the CALIPSO Lidar measurements, *J. Atmos. Ocean. Tech.*, 26, 2034–2050, doi:10.1175/2009JTECHA1228.1, 2009.
- Vernier, J. P., Pommereau, J. P., Garnier, A., Pelon, J., Larsen, N., Nielsen, J., Christensen, T., Cairo, F., Thomason, L. W., Leblanc, T., and McDermid, I. S.: Tropical stratospheric aerosol layer from CALIPSO lidar observations, *J. Geophys. Res.*, 114, D00H10, doi:10.1029/2009JD011946, 2009.
- Wandinger, U., Tesche, M., Seifert, P., Ansmann, A., Müller, D., and Althausen, D.: Size matters: Influence of multiple scattering on CALIPSO light-extinction profiling in desert dust, *Geophys. Res. Lett.*, 37, L10801, doi:10.1029/2010GL042815, 2010.
- Weisz, E., Li, J., Menzel, W. P., Heidinger, A. K., Kahn, B. H., and Liu, C. Y.: Comparison of AIRS, MODIS, CloudSat and CALIPSO cloud top height retrievals, *Geophys. Res. Lett.*, 34, L17811, doi:10.1029/2007GL030676, 2007.
- Welton, E. J., Voss, K. J., Gordon, H. R., Maring, H., Smirnov, A., Holben, B., Schmid, B., Livingston, J. M., Russell, P. B., Durkee, P. A., Formenti, P., and Andreae, M. O.: Ground-based lidar measurements of aerosols during ACE-2: Instrument description, results, and comparisons with other ground-based and airborne measurements, *Tellus B*, 52, 636–651, doi:10.1034/j.1600-0889.2000.00025.x, 2000.

- Winker, D. M.: Accounting for multiple scattering in retrievals from space lidar, in Proc. SPIE: 12th International Workshop on Lidar Multiple Scattering Experiments, edited by: Werner, C., Oppel, U. G., and Rother, T., 5059, 128–139, doi:10.1117/12.512352, 2003.
- Winker, D. M., Vaughan, M. A., Omar, A., Hu, Y., Powell, K. A., Liu, Z., Hunt, W. H., and Young, S. A.: Overview of the CALIPSO mission and CALIOP data processing algorithms, *J. Atmos. Ocean. Tech.*, 26, 2310–2323, doi:10.1175/2009JTECHA1231.1, 2009.
- Winker, D. M., Pelon, J., Coakley Jr., J. A., Ackerman, S. A., Charlson, R. J., Colarco, P. R., Flamant, P., Fu, Q., Hoff, R., Kitatake, C., Kubar, T. L., LeTreut, H., McCormick, M. P., Megie, G., Poole, L., Powell, K., Trepte, C., Vaughan, M. A., and Wielicki, B. A.: The CALIPSO Mission: A Global 3D View Of Aerosols And Clouds, *B. Am. Meteorol. Soc.*, 91, 1211–1229, doi:10.1175/2010BAMS3009.1, 2010.
- Wu, D., Wang, Z., Wang, B., Zhou, J., and Wang, Y.: CALIPSO validation using ground-based lidar in Hefei (31.9° N, 117.2° E), China, *Appl. Phys. B*, 102, 185–195, doi:10.1007/s00340-010-4243-z, 2011.
- Yorks, J., Hlavka, D., Vaughan, M., McGill, M., Hart, W., Rodier, S., and Kuehn, R.: Airborne Validation of Cirrus Cloud Properties Derived from CALIPSO Lidar Measurements: Spatial Properties, *J. Geophys. Res.*, 116, D19207, doi:10.1029/2011JD015942, 2011.
- Young, S. A. and Vaughan, M. A.: The retrieval of profiles of particulate extinction from Cloud-Aerosol Lidar Infrared Pathfinder Satellite Observations (CALIPSO) Data: Algorithm Description, *J. Atmos. Oceanic Technol.*, 26, 1105–1119, doi:10.1175/2008JTECHA1221.1, 2009.